Published in final edited form as:
Acta Biomater. 2015 March ; 14: 84–95. doi:10.1016/j.actbio.2014.11.035.

Cardiac Extracellular Matrix-Fibrin Hybrid Scaffolds with Tunable Properties for Cardiovascular Tissue Engineering

Corin Williams[1], **Erica Budina**[1,#], **Whitney L. Stoppel**[1], **Kelly E. Sullivan**[1], **Sirisha Emani**[2], **Sitaram M. Emani**[2], and **Lauren D. Black III**[1,3,*]

[1]Department of Biomedical Engineering, Tufts University, 4 Colby St, Medford, MA 02155 USA

[2]Department of Cardiac Surgery, Boston Children's Hospital, 300 Longwood Ave, Boston, MA 02115 USA

[3]Cellular, Molecular and Developmental Biology Program, Sackler School for Graduate Biomedical Sciences, Tufts University School of Medicine, 145 Harrison Ave, Boston, MA 02111, USA

Abstract

Solubilized cardiac extracellular matrix (ECM) is being developed as an injectable therapeutic that offers promise for promoting cardiac repair. However, the ECM alone forms a hydrogel that is very soft compared to the native myocardium. As both the stiffness and composition of the ECM are important in regulating cell behavior and can have complex synergistic effects, we sought to develop an ECM-based scaffold with tunable biochemical and mechanical properties. We used solubilized rat cardiac ECM from two developmental stages (neonatal, adult) combined with fibrin hydrogels that were crosslinked with transglutaminase. We show that ECM was retained within the gels and Young's modulus could be tuned to span the range of the developing and mature heart. C-kit+ cardiovascular progenitor cells from pediatric patients with congenital heart defects were seeded into the hybrid gels. Both the elastic modulus and composition of the scaffolds impacted the expression of endothelial and smooth muscle cell genes. Furthermore, we demonstrate that the hybrid gels are injectable, and thus have potential for minimally invasive therapies. ECM-fibrin hybrid scaffolds offer new opportunities for exploiting the effects of both composition and mechanical properties in directing cell behavior for tissue engineering.

[*]*Corresponding author:* Lauren D. Black, III, Tufts University, Department of Biomedical Engineering, 4 Colby St, Medford, MA 02155, Fax: 617-627-3231, lauren.black@tufts.edu.
[#]Current affiliation: School of Engineering and Applied Sciences, 29 Oxford St, Cambridge, MA 02138, USA

Disclosures
None.

Keywords

biomimetic material; cardiac tissue engineering; extracellular matrix; fibrin; mechanical properties; progenitor cell

1. Introduction

Eight in every one thousand infants are born with a congenital cardiovascular disorder [1]. These include various cardiomyopathies, congenital heart defects (CHDs), or arrhythmias that can lead to heart failure at a young age [2]. Currently, the majority of available therapies are geared toward slowing down the progression of heart failure and not toward restoring the proper contractile function of the myocardium [3]. For patients with end stage heart failure, heart transplantation is the only successful long-term option. However, there is a shortage of available donor organs for pediatric patients and mortality on the waiting list is high [4, 5]. Furthermore, patients who receive a heart transplant are subject to potentially serious post-surgery side effects and lifelong immune suppression therapies [4]. Thus, there is a great need for the development of alternative strategies to treat CHDs and heart failure in the young.

Recently, c-kit+ cardiovascular progenitor cells (CPCs) have gained much attention for their potential to improve heart function after myocardial infarction in adults [6]. CPCs can also be isolated from young patients with various CHDs and differentiated into the three cardiovascular lineages of the heart: endothelial cells, vascular smooth muscle cells, and cardiomyocytes [7]. In addition, the regenerative potential of CPCs from infants is greater than adult CPCs [8], suggesting that c-kit+ CPCs may be a promising cell source for cardiovascular tissue engineering or regenerative medicine strategies to treat pediatric patients. However, the efficiency of directed differentiation of CPCs with established protocols is low (~1% or less for all three cell types) [7]. A recent study suggests that although c-kit+ cells do not contribute significantly to the cardiomyocyte population *in vivo*, they are highly capable of generating cardiac endothelial cells [9]. Promoting vascularization of damaged tissue and endothelial cell-cardiomyocyte communication are key factors in cardiac repair [10]. The development of biomaterials that promote cardiovascular differentiation of CPCs would greatly enhance their regenerative potential for future therapies.

Recent studies point to a critical role of the extracellular matrix (ECM) in stem cell differentiation. In particular, the composition and mechanical properties of the ECM can influence stem cell fate. For example, human pluripotent stem cells showed robust cardiac differentiation when established growth factor-based protocols were used in combination with culture on Matrigel [11]. Adult rat c-kit+ CPCs had higher expression of cardiac genes when cultured on adult porcine cardiac ECM compared to Collagen I [12]. The stiffness of the substrate alone was found to drive mesenchymal stem cells towards neurogenic, myogenic, or osteogenic fates [13], and chick embryonic cardiac cells showed increased maturation when cultured on hydrogels that stiffened over time in culture [14]. The above studies have been carried out in 2D; however, the complex functionality of cells can be lost

or altered when cultured on planar surfaces [15]. Furthermore, the effect of substrate stiffness and composition on the cardiovascular fate of c-kit+ cells (i.e., endothelial and smooth muscle cell lineages) has not been investigated.

Solubilized cardiac ECM shows promise as an injectable biomaterial for repair of myocardial infarction [16-18]. Solubilized ECM can reform a 3D naonfibrous hydrogel at physiological pH and temperature [16]. However, ECM hydrogels have a limited range of mechanical properties that do not match the native myocardium, and since they are very soft and rapidly degraded, pure ECM hydrogels cannot be used for 3D cell encapsulation [19]. Thus, the aim of this work was to create cardiac ECM-fibrin hybrid scaffolds with tunable composition and elasticity in order to mimic properties of the native myocardium during development and maturation. Fibrin is commonly used for tissue engineering [20-23] and it is also highly angiogenic [24-26]; thus, by combining cardiac ECM and fibrin our long-term goal is to promote both vascular and cardiac differentiation within the same scaffold, and further modulate cell response by tuning scaffold stiffness. Solubilized cardiac ECM from neonatal or adult rat hearts was incorporated into fibrin gels and scaffold stiffness was altered via crosslinking with transglutaminase (TG). CPCs from pediatric patients had good viability within the scaffolds and interacted with and remodeled the ECM over time in culture. Gene expression at 21 days showed that endothelial and smooth muscle markers were influenced by ECM developmental age and scaffold elastic modulus. Furthermore, these scaffolds are injectable through a 25G needle and thus may be beneficial for minimally invasive cell delivery in future applications.

2. Materials and Methods

2.1. ECM Isolation and Solubilization

All animal procedures were performed in accordance with the Institutional Animal Care and Use Committee at Tufts University and the NIH Guide for the Care and Use of Laboratory Animals. ECM was isolated and solubilized according to previously published methods [27]. Briefly, hearts were harvested from euthanized P2-P3 neonatal pups and adult female Sprague Dawley rats (Charles River Laboratories). The ventricular tissue was minced and decellularized using 0.5% or 1% (wt/vol) sodium dodecyl sulfate (SDS) in deionized water (neonatal or adult hearts, respectively) with gentle shaking for 1-2 days until decellularization was complete. The ECM was transferred to a 0.5% or 1% TritonX-100 (vol/vol) solution for ~ 4-8 hr to remove SDS and then washed with deionized water at least 3 times for 12-24 hr per wash. The ECM was frozen at −20°C, lyophilized for 24 hours, and solubilized at a concentration of 10 mg/ml in 1 mg/ml pepsin dissolved in 0.1 M HCl (4-6 hr or 24-48 hr for neonatal or adult hearts, respectively). Immediately prior to use, the cardiac ECM solution was neutralized to pH 7 with 1 N NaOH.

2.2. Preparation of Transglutaminase Stock Solutions

Two separate stock solutions of transglutaminase (TG; 60 μg/ml and 600 μg/ml) were prepared fresh for each experiment. First, a 5 mg/ml solution was prepared by dissolving TG (Ajinomoto, Chicago, IL) in 20 mM HEPES buffer. The 5 mg/ml solution was then further diluted in 20 mM HEPES to create the 60 μg/ml stock solution (used for final concentrations

of 1.2 and 12 μg/ml TG in the gels) and the 600 μg/ml stock solution (used for a final concentration of 120 μg/ml TG in the gels).

2.3. Preparation of ECM Only Hydrogels

ECM hydrogels were prepared using various concentrations of TG (0, 1.2, 12, and 120 μg/ml). Decellularized ECM solution was neutralized and diluted to 6 mg/ml [16] before adding TG, vortexed briefly, and then pipetted into 15 × 15 × 5 mm Tissue-Tek cryomolds (Ted Pella, Inc). Samples were incubated at 37°C for approximately 30 min. Collagen I (BD Biosciences) at the same concentration was used as a control.

2.4. Preparation of ECM-Fibrin Hydrogels Crosslinked by Transglutaminase

ECM-fibrin hybrid scaffolds were prepared using the various concentrations of TG described above. The gel solution was composed of fibrinogen (33 mg/ml stock, Sigma) at a final concentration of 3.3 mg/ml, 20 mM HEPES buffer, Dulbecco's Modified Eagle Medium (DMEM) (Invitrogen), thrombin (25 U/ml stock, Sigma) at a final concentration of 0.425 U/ml, calcium (1M stock, Sigma) at a final concentration of 1.3 mM, and cardiac ECM (2 mg/ml stock) at a final concentration of 340 μg/ml. In preliminary experiments, we found that higher concentrations of ECM inhibited the polymerization of fibrin (data not shown). The gel solution was mixed by gentle inversion, pipetted into molds or well plates, and allowed to gel at 37°C prior to carrying out the experiments described below.

2.5. Uniaxial Mechanical Testing

ECM-fibrin hydrogels were prepared as described above and pipetted into 15 × 15 × 5 mm cyromolds (300 μl per mold, six molds per condition) which were pre-coated in 5% pluronics solution to facilitate removal of the gels from the molds. The samples were allowed to gel for 30 min at 37°C, removed from the molds and incubated in PBS at 37°C overnight. For uniaxial testing, the hydrogels were removed from the 6-well plate and the excess PBS was gently removed using a Kim wipe™. Custom-made aluminum clamps were attached to each end of the hydrogel using super glue. An image of the sample's thickness was acquired using a custom-built device. The sample was then transferred to a PBS bath and attached to the custom-built uniaxial stretcher, as previously described [28, 29]. Prior to stretching, the sample's initial length and width were determined using a digital caliper (Fisher Scientific). A custom-written LabVIEW program then applied a triangle waveform to stretch the sample to 25% strain. Each sample was pre-conditioned for at least 5 cycles before recording the force and length data. A stress-strain curve was generated for each sample, and the Young's modulus was determined by calculating the slope in the linear region of the curve between 15 and 20 % strain.

2.6. Swelling Test

Samples were prepared as described above for uniaxial stretching. After incubating in PBS overnight, excess fluid was carefully removed from the gels with a Kim wipe™. The mass of each swollen hydrogel (Ms) was determined using an electronic balance. The samples were transferred into individual microcentrifuge tubes and frozen at −20°C for 24 hours. The samples were then placed in a lyopholizer (Labconco, Kansas City, MO) for 24 hours until

fully dry. The mass of each dry gel (Md) was determined using an electronic balance. Percent swelling (% S) was calculated using the following formula [30]:

$$\%S = \frac{M_s - M_d}{M_d} * 100$$

2.7. ECM Retention Studies Using Fluorescently Labeled ECM

To examine ECM retention within the hybrid gels, fluorescently labeled ECM was used. Alexa Fluor 488 dye (Invitrogen) was dissolved in dimethyl sulfoxide (DMSO) to a concentration of 5 mg/ml. The ECM was neutralized and diluted to 1 mg/ml in 0.1 M sodium bicarbonate buffer at pH 8.3. The ECM (1 mg total) was reacted with 5 μl of the dye for 1 hour at room temperature (RT) with end-over-end mixing, and then stored in the dark at 4°C. The fluorescent ECM-fibrin gels were prepared the following day as described above. At 1 hr after polymerization, fluorescence readings of the gels were obtained using a spectrophotometer (499 nm excitation, 519 nm emission). The gels were then covered with PBS and incubated for 1 week at 37°C. The PBS on the surface of the gels was removed and the fluorescence readings were repeated to determine the levels within the gels. Fluorescence readings at 1 wk were normalized to their respective 1 hr baseline levels, assuming the signal was 100%. In addition, we studied ECM release into the culture medium in the presence of cells. Hybrid gels containing fluorescently labeled ECM, with or without cells, were monitored over several days. The media was refreshed each day and the fluorescence signal in the collected media was read on the spectrophotometer. Cell interactions with the labeled ECM were studied qualitatively via fluorescence microscopy. Cells were seeded into the gels as described below and imaged at 2, 4, 14, and 21 days.

2.8. Isolation, Culture, and Characterization of c-kit+ Cardiovascular Progenitor Cells

This study was approved by the Institutional Review Boards at Boston Children's Hospital and Tufts University. De-identified, discarded tissue samples from the right atrial appendage were collected from pediatric patients undergoing cardiac surgery at Boston Children's Hospital (***Supplementary Table 1***). Cells were isolated from the atrial tissue using a series of digestions in Collagenase type 2 (Worthington Biochemical Corp, Lakewood, NJ) dissolved in PBS supplemented with 20 mM glucose. After each digestion, the supernatant was collected and the digestion was "stopped" using 5% fetal bovine serum (FBS) in DMEM. After the digestion was complete, the cell pellet was spun down at 1700 rpm for 5 min. The pellet was re-suspended in Ham's F-12 Nutrient Mix supplemented with 1x Insulin-Transferrin-Selenium and 1% penicillin-streptomycin (all from Invitrogen). CPCs were purified and cultured similar to previously described methods [12]. A rabbit polyclonal c-kit antibody (clone H-300, Santa Cruz) pre-conjugated to magnetic beads (Dynabeads M-280 sheep anti-rabbit IgG, Invitrogen) was added to the cells and incubated for 2 hr at 37°C with gentle agitation. The c-kit+ CPCs were then isolated by magnetic sorting (DynaMag-15, Invitrogen). We did not perform a second sorting for hematopoietic lineage markers ("lineage depletion"), as a previous study demonstrated it was unnecessary [31]. CPCs were maintained in Ham's F-12 Nutrient Mix supplemented with 10% FBS (Hyclone, ES grade) and 1% penicillin-streptomycin, with 10 ng/ml FGF-2 (PeproTech) added fresh at each

feeding. Cells were characterized at passage 4 (the same passage used for experiments) by immunocytochemical staining for the following markers: c-kit (same as above), GATA4 (clone H-112, Santa Cruz), Nkx2.5 (clone H-114, Santa Cruz), PECAM-1 (clone 10G9, Santa Cruz), smooth muscle α-actin (SMA) (clone 1A4, Santa Cruz), CD34 (clone ICO115, Santa Cruz), and cardiac Troponin I (cTnI) (ab47003, Abcam). Proliferation was assessed by staining for Ki67 (ab15580, Abcam) and Aurora B Kinase (clone 6/AIM-1, BD Biosciences).

2.9. CPC Differentiation on ECM

To determine the effects of ECM alone on c-kit+ cell differentiation, cells were cultured on ECM coated tissue culture polystyrene (TCPS). Neonatal and adult ECM were digested as described above and coated onto 12-well plates at a density of 50 μg/cm^2, similar to our previously described studies [27]. Poly-L-lysine (PLL) (0.01% solution, Sigma) was used as a control substrate. The substrates were dried overnight in a sterile tissue culture cabinet and washed once with PBS prior to cell seeding. CPCs were harvested from T75 flasks using TrypLE Select (Invitrogen) for 3 min and spun down at 1500 rpm for 5 min. The cells were resuspended in a small volume of DMEM and counted with a hemocytometer. Cells were then seeded onto the PLL or ECM-coated substrates in “Differentiation Medium” (50/50 Ham’s F-12 Nutrient Mix/Iscove’s Modified Dulbecco’s Medium, 2% horse serum, 1X MEM non-essential amino acids, 1X Insulin-Transferrin-Selenium, and 1% penicillin-streptomycin) [32] supplemented with 10 ng/ml FGF-2 and 25 ng/ml IGF-1 (PeproTech) added fresh at each feeding. All experiments were performed with CPCs at passage 4.

After 21 days of culture, RNA was isolated using the RNeasy Mini Kit (Qiagen) per the manufacturer’s instructions. RNA was stored at −80°C until reverse transcription was performed using the Applied Biosystems High Capacity Reverse Transcription Kit. The resulting cDNA was stored at −20°C until use. Quantitative PCR was then carried out using the Stratagene Mx3000P qPCR System (Agilent Technologies). The following genes were assayed using TaqMan primers from Life Technologies: PECAM1, PCDH12 (VE-Cadherin-2), ACTA2 (smooth muscle α-actin), CNN1 (basic calponin), TTN (titin), and GAPDH (***Supplementary Table 2***). Genes of interest were normalized to GAPDH expression and the comparative C_T method was used with PLL conditions as controls. Genes with approximately 2-fold change or greater were identified and statistical analysis was performed as described below (N = 3-4 for each condition).

2.10. Cell Seeding within Hybrid Gels

To assess CPC behavior in the ECM-fibrin hybrid gels, cells were harvested from T75 flasks, counted, and added to the ECM-fibrin gel solution at a final concentration of 700,000 cells/ml. The cell-gel mixture was then immediately pipetted into 96-well plates (75 μl per well) or 48-well plates (250 μl per well) and allowed to gel for 30 min prior to adding media. For the experiments described below, cells in ECM-fibrin gels were cultured in Differentiation Medium up to 21 days.

2.11. Immunostaining and Imaging within 3D Scaffolds

Immunostaining was used to assess cell morphology and make measurements over time within the ECM-fibrin gels. Briefly, samples were fixed at 1, 7, and 21 days in 4% paraformaldehyde (PFA) for 2 hr at 4°C. Cells were permeabilized with 0.1% TritonX-100 in PBS for approximately 30 min at room temperature and then blocked with 5% donkey serum and 1% bovine serum albumin (BSA) in PBS for 2 hr at 37°C. Actin fibers and nuclei were stained using TRITC-labeled Phalloidin (Sigma) and Hoechst 33342 (Invitrogen), respectively, for 2 hr at 37°C. Samples were washed several times with PBST and then imaged using an Olympus IX81 microscope equipped with spinning disk confocal and Metamorph Basic software (version 7.7.4.0, Molecular Devices).

2.12. Cell Measurements

A cell viability assay was performed at 1 day using the Molecular Probes Live/Dead Kit according to the manufacturer's instructions. In a preliminary experiment, we found that the ethidium homodimer ("dead") stain did not produce accurate readings due to autofluorescence of the gels in the same wavelength range (data not shown); therefore, only the calcein AM ("live") stain was used. The samples were washed twice with PBS and then 200 μl of 4 mM calcein AM solution was added to each gel. After 2 hr, fluorescence readings were obtained at 530 nm (excitation at 490 nm). The fibrin only condition was treated as a positive control for cell viability. The scaffolds were then fixed with 4% PFA and stained with Hoechst 33342 nuclear dye. Random images of cell nuclei were acquired for each sample and cell density was determined using a custom-written pipeline in CellProfiler (version r11710, The Broad Institute, Cambridge, MA), similar to previously described methods [27].

Fold changes in cell numbers and network formation at 1 wk were also assayed by image analysis. Cell numbers were measured at 1 and 7 days using CellProfiler and the fold change was calculated. To measure network formation, a "Network Maturity Level Score" [24] was applied to images of F-actin staining as follows: 1 – individual cells; 2 – groups of non-interconnected cells; 3 – partially connected networks of cells; 4 – full connected networks of cells.

2.13. Gene Expression at 21 Days

Gene expression profiles for various cardiovascular differentiation markers were determined at 21 days using custom-designed PCR array plates from SA Biosciences and the genes described above for the ECM studies (***Supplementary Table 2***). For the PCR array plates, RNA was isolated using the RNeasy Mini Kit (Qiagen) per the manufacturer's instructions. RNA was stored at −80°C until reverse transcription was performed using the RT^2 First Strand Kit (Qiagen) and the resulting cDNA was stored at −20°C until use. Quantitative PCR was carried out in the array plates per the manufacturer's instructions using the Stratagene Mx3000P qPCR System. To determine the effects of stiffness on gene expression, the comparative C_T method was used with fibrin only conditions as controls. Genes with approximately 2-fold change or greater were identified and statistical analysis was performed as described below (N = 3-4 for each condition).

2.14. Injectability Study

To demonstrate that TG-crosslinked ECM-fibrin scaffolds have potential as an injectable therapeutic, gel solutions were prepared as described above with 5 μ l blue food dye added to visualize the gels. The solution was drawn up into a syringe using a 25G needle and injected into the left ventricular free wall of an adult rat heart *ex vivo*. The solution was also injected subcutaneously in a euthanized rat and allowed to gel for 20 min. Macroscopic images were acquired using a Nikon digital camera.

2.15. tatistical Analysis

Statistical significance was determined using the appropriate dimension of analysis of variance and Tukey's posthoc test in SigmaPlot 12.0 software. The Student's t-test was used for pair-wise comparisons. Differences were considered statistically significant for $p < 0.05$.

3. Results

3.1. Development and Characterization of ECM-Fibrin Hybrid Gels

We first attempted to make hydrogel scaffolds composed solely of cardiac ECM. Although it has been reported that cardiac ECM can spontaneously gel when brought to physiological pH and temperature [16], the gels are orders of magnitude softer than native myocardium [33-35]. We also found that the ECM only gels lacked significant mechanical strength and therefore we tested whether the addition of crosslinking agents could improve ECM scaffold integrity. We added TG at various concentrations and found some improvement in gelation and fiber formation (***Figure 1A***); however, even at the highest concentration of TG, the ECM gels appeared incompletely crosslinked and remained a viscous fluid. TG did not have any apparent effect on Collagen I controls (***Figure 1A***). We also attempted to crosslink ECM with genipin [36] and ribose [37] with similar results (data not shown). Therefore, we concluded that in order to improve the mechanical properties of our ECM-based scaffold to a range comparable to native myocardium, the addition of another material would be necessary.

Fibrin is an FDA-approved biomaterial that is also well-established as a scaffold for cardiac tissue engineering [21]. In addition, fibrin can promote vascularization [26] and can be further crosslinked by TG [38]. Therefore, we developed ECM-fibrin hybrid scaffolds (***Figure 1A***) with tunable mechanical properties. Uniaxial stretching was performed to determine the impact of increasing TG on the Young's modulus (elasticity) of the scaffolds. Fibrin only scaffolds had a Young's Modulus of 2.7 ± 1.3 kPa; the addition of ECM did not significantly affect the mechanical properties of the gels (***Figure 1B***). The addition of 12 μg/ml TG to the ECM-fibrin scaffolds resulted in an increase in Young's modulus to 13.7 ± 4.8 kPa, which was significantly greater than fibrin and ECM-fibrin scaffolds without TG. Scaffolds with 120 μg/ml TG had a Young's modulus of 32 ±4.6 kPa, which was significantly increased over all other conditions. Of note, these elastic moduli span the range that we and others have previously determined for developing and mature rodent myocardium [34, 35]. Crosslinking with TG was further confirmed by the swelling test (***Figure 1C***). Samples without TG had significantly higher swelling ratios, which decreased with increasing TG. Furthermore, we found a strong correlation ($R^2 = 0.98$) between the

Young's Modulus and the swelling ratio using a power law fit (***Figure 1D***). We will subsequently refer to the gels by their composition and elasticity: fibrin 2 kPa (0 TG), ECM-fibrin 2 kPa (0 TG), ECM-fibrin 8 kPa (1.2 μg/ml TG), ECM-fibrin 14 kPa (12 μg/ml TG), and ECM-fibrin 32 kPa (120 μg/ml TG).

3.2. ECM Retention in Hybrid Gels

As our initial experiments suggested that TG may not fully crosslink ECM, it was necessary to determine whether the ECM would be retained within the hybrid scaffolds over time. To characterize ECM retention, ECM was labeled with the fluorescent dye Alexa Fluor 488 and incorporated into the fibrin scaffolds; scaffolds with non-labeled ECM were used as controls for background fluorescence. Immediately after gelation and before the addition of PBS, fluorescence readings were similar in all fluorescently labeled samples regardless of TG crosslinking (***Figure 2A***). PBS was then added to the gels and incubated at 37°C for 1 wk; fluorescence readings were then repeated for the gels. Although there was some loss of ECM into the PBS, the fluorescence readings within the gels were still approximately 70% of the 1 hr baseline, suggesting that most of the ECM had been retained within the gels. Furthermore, ECM retention was independent of TG crosslinking, meaning that there would be no need to adjust the ECM concentrations for each of the gel formulations for subsequent cell experiments. Finally, we also studied ECM release in the presence of cells and found that it was not significantly different compared to gels without cells (***Supplementary Figure 1***).

To study cell interactions with the ECM, CPCs were cultured in fluorescently labeled ECM-fibrin scaffolds for 21 days. Over time, the ECM became more concentrated and the formation of fluorescent ECM fibers was gradually observed around cells (***Figure 2B***). Cell interactions with ECM did not appear to be affected by ECM developmental age or scaffold stiffness. Furthermore, changes in ECM structure were not observed in the absence of cells: the fluorescence signal remained uniform throughout the gels over time (data not shown). Taken together, our results indicate that ECM is retained within the hybrid gels regardless of TG crosslinking and that cells can interact with and remodel the ECM.

3.3. Characterization of c-kit+ Cardiovascular Progenitor Cells

C-kit+ CPCs were successfully isolated from pediatric patients with various types of CHDs (***Supplementary Table 1***). The cells were highly proliferative with a doubling time of ~25-30 hr. Staining for the mitosis marker Ki67 revealed that 90% of the cells were proliferating at passage 4 and approximately 50% confluence. The cytokinesis marker Aurora B Kinase (ABK) was present in 5% of the cells (***Figure 3A***).

In general, we found that at least up to passage 8, the cells remained 90% c-kit+ or greater as determined by flow cytometry and/or immunostaining (***Figure 3B, Supplementary Figure 2A***). At passage 4, 28% and 79% the CPCs expressed the early cardiac markers Nkx2.5 and GATA4, respectively (***Figure 3B, Supplementary Figure 2B-D***). About 50-60% of the cells expressed the endothelial markers PECAM-1 and vWF. Only a small percentage of the cells were positive for the smooth muscle marker SMA (2.6%) and the hematopoietic marker CD34 (1%). Some cells also expressed VEGFR2 (~20%; ***Figure 3B***). At passage 14,

staining suggested spontaneous differentiation towards the three cardiovascular lineages as indicated by increased numbers of cells expressing PECAM-1 and SMA, and a few cTnI+ cells (***Figure 3C***). Taken together, our data suggested that the isolated c-kit+ cells had potential for cardiovascular differentiation and a natural propensity for the endothelial cell lineage in particular, as others have shown [9]. Moreover, the high expression of PECAM-1 and GATA4 indicates a possible population of doubly labeled cells. Previous studies have indicated that these cells do exist in cardiac development and are likely progenitors that give rise to both endocardial and myocardial cells [39]. We studied their behavior on ECM alone and in our ECM-fibrin scaffolds in subsequent experiments.

3.4. Differentiation on ECM

To determine the effects of ECM alone on c-kit+ CPC differentiation, cells were cultured on PLL, neonatal ECM and adult ECM-coated TCPS for 21 days. There was a general trend in increased cardiovascular gene expression on ECM compared to PLL controls. However, the only significant differences observed were for ACTA2 and CNN1, which increased approximately 4-5 fold on adult ECM compared to PLL controls and neonatal ECM (***Figure 4***). These data suggest that adult ECM promotes smooth muscle differentiation of pediatric c-kit+ CPCs.

3.5. Cell Measurements in ECM-Fibrin Hybrid Gels

We next evaluated the effect of ECM-fibrin hybrid gels on c-kit+ CPCs. Cells were seeded into ECM-fibrin scaffolds that contained either neonatal cardiac ECM or adult cardiac ECM and crosslinked with TG. At 24 hr, we assessed cell viability and density to determine if either ECM type or crosslinking had any negative effects on the cells. Cell viability was significantly lower in neonatal ECM-fibrin scaffolds with 14 kPa (12 μg/ml TG) and 32 kPa (120 μg/ml TG) elastic moduli compared to 2 kPa fibrin and ECM-fibrin scaffolds (0 TG), but still acceptable at 80%. Cell viability in adult ECM-fibrin gels was similar to fibrin only controls regardless of elastic modulus (***Figure 5A***). At 24 hr, cell density was significantly higher in fibrin only controls compared to all other conditions (***Figure 5B***). At 1 wk, there was a modest, but significant, increase in cell numbers in soft adult ECM-fibrin gels (2 kPa and 8 kPa) compared to fibrin 2 kPa control gels (***Figure 5C***). Cell numbers were similar in neonatal ECM gels for all elastic moduli studied. We also found that Young's modulus, but not ECM age, affected network formation in the hybrid gels. Softer gels (2 kPa) had significantly higher network maturity scores compared to the two stiffest ECM-fibrin gels (14 kPa and 32 kPa) (***Figure 5D***). This data suggests that softer gels promoted network formation while stiffer gels inhibited it. Representative images of the cell networks for each gel stiffness are shown in ***Figure 6***.

3.6. Gene Expression in ECM-Fibrin Hybrid Gels

After 21 days of culture within ECM-fibrin gels, we analyzed a panel of genes via PCR that included various cardiovascular differentiation markers. To elucidate the effects of stiffness on differentiation, data was normalized to the fibrin only controls. The expression of KIT (c-kit) was not affected by ECM age or stiffness (***Figure 7A***). The addition of neonatal ECM in 2 kPa gels significantly down-regulated VWF (endothelial cell marker); however, the

expression levels returned to that of the fibrin only controls at the higher Young's modulus values (***Figure 7B***). In contrast, adult ECM led to significant up-regulation of VWF at the highest stiffness investigated (***Figure 7 B***). CNN1 (smooth muscle marker) was up-regulated 2-fold in 32 kPa neonatal ECM-fibrin gels compared to 8 kPa ECM-fibrin gels and 2 kPa fibrin controls (***Figure 7C***). However, CNN1 expression remained constant in adult ECM-based gels. TTN (cardiac marker) was down-regulated at intermediate elasticity (8 kPa) compared to 2 kPa fibrin controls for both neonatal and adult ECM-based gels (***Figure 7D***). We did not observe significant differences in PECAM1, PCDH12, ACTA2, TAGLN, GATA4, or TNNT1 (***Supplementary Figure 3***). Overall, these data demonstrate a complex interplay of ECM composition and elastic modulus in affecting the expression of VWF and CNN1 genes in CPCs.

3.7. Feasibility of Injection of ECM-Fibrin Scaffolds

There has been significant interest in using cardiac ECM as an injectable therapeutic [17, 18, 40, 41]. However, ECM alone produces a very soft hydrogel that does not match the mechanical properties of the native myocardium. To demonstrate that our ECM-fibrin hybrid was injectable, we prepared solutions with a small amount of blue food dye to easily visualize the gels. Even the stiffest formulation was easily drawn into a syringe with a 25G needle (***Figure 8A***) and could be injected into the ventricular myocardium (***Figure 8B***) and subcutaneously (***Figure 8C***). The ECM-fibrin solution could be maintained in the syringe for 5-10 min for various injections. Twenty minutes post-injection, an incision was made in the skin to reveal a clearly defined gel (***Figure 8D***).

4. Discussion

One of the most important and challenging aspects of biomimetic scaffold design for tissue engineering and regenerative medicine is recapitulating the complex biochemical and mechanical cues of the native tissue. Many attempts to create engineered cardiac tissue have focused on synthetic materials, non-mammalian materials such as alginate or chitosan, or single proteins such as collagen I or fibrin [42]. However, the cardiac ECM is comprised of a complex and specific mixture of proteins, and this composition changes throughout heart development and maturation [14, 27, 43, 44]. In addition, the mechanical properties of tissues can play a critical role in directing cell response [13, 14, 45, 46], and the interplay between ECM composition and stiffness has only recently begun to be appreciated [34, 47-49]. Therefore, we sought to develop a cardiac ECM-based scaffold that could be tuned to mimic both the complex composition and stiffness of the myocardium during development and maturation.

Solubilized cardiac ECM has proven to be especially promising as an injectable therapeutic which could allow for the tuning of scaffold properties and for the formation of cell-laden hydrogels *in situ*. However, there are several challenges to using the cardiac ECM alone as a scaffold. Solubilized ECM forms a hydrogel with stiffness of ~5 Pa [33] while the native myocardium is in the kPa range [34, 35]. Crosslinking the ECM hydrogel with glutaraldehyde can increase stiffness to 136 Pa [33]; however, this is still far below the native tissue and the cytotoxic effects of glutaraldehyde are not desirable for cell-based

applications. In our initial experiments, we explored several milder cross-linking agents (ribose, genipin, and TG) to further improve the mechanical properties of ECM only gels with limited to no success (data not shown). This led us to explore the option of creating a hybrid scaffold. We chose fibrin as an additional biomaterial because it is biocompatible, biodegradable, and its mechanical properties can be easily tuned. We then pursued TG as our crosslinking agent because it is also highly biocompatible and is able to crosslink fibrin [38, 50]. Our results demonstrated that the addition of ECM alone did not affect fibrin mechanics while increasing TG led to increasing elastic modulus (***Figure 1***) in the range of the developing and mature rat myocardium [34]. ECM was retained within the hybrid gels and c-kit+ CPCs seeded into the gels were able to interact with and remodel the ECM over time in culture. (***Figure 2***). Furthermore, cell viability was high in the gels (80% or better compared to fibrin only controls), particularly when compared to the use of other crosslinking agents such as glutaraldehyde and genipin, which are cytotoxic even at relatively low concentrations. We did note that cell viability was significantly lower in neonatal ECM gels with 12 and 120 μg/ml TG (14 kPa and 32 kPa) compared to fibrin only (2 kPa, no TG) while viability was unaffected by TG cross-linking in adult ECM gels (***Figure 5A***). This suggests that the adult cardiac ECM was better at promoting cell survival, but the specific factors would have to be identified in future studies.

We found that CPC differentiation was affected by both the stiffness and the composition of the cardiac ECM-fibrin hybrid gels. Furthermore, gene expression was different on ECM alone vs. within ECM-fibrin scaffolds. For example, we found that adult ECM alone significantly up-regulated smooth muscle cell genes (ACTA2 and CNN1) (***Figure 4***), but these genes were unaffected in the adult ECM-fibrin hybrid (***Figure 7C, Supplementary Figure 3C***). Although the concentration of fibrin was roughly 10 times higher than the ECM (3.3 mg/ml vs. 340 μg/ml), the ECM still had a significant influence on the cells. Most striking was the effect on gene expression for VWF, a marker for endothelial cell differentiation. The addition of neonatal cardiac ECM led to down-regulation of VWF which then normalized to fibrin only controls with increasing stiffness. However, in adult ECM-based gels, VWF gene expression was up-regulated with increasing stiffness to a 6-fold increase above fibrin only controls in the stiffest condition studied (~32 kPa) (***Figure 7B***). Of additional note, while stiff adult ECM gels promoted vWF expression (endothelial marker) and stiff neonatal ECM gels promoted CNN1 expression (smooth muscle marker), network formation was better in softer gels regardless of ECM (***Figure 5D***). It is intriguing to consider that the biochemical and biomechanical signals which promote differentiation and maturation may be different, and warrant further exploration.

Other studies have shown that mechanical forces and matrix composition can affect endothelial cell behavior. For example, laminin-based peptides can promote tubulogenesis [51], and we have found that laminins are more abundant in the adult rat heart than in the neonatal heart [27]. Adult porcine ECM can promote vascularization in a rat model of myocardial infarction [16]. Others have shown that endothelial cells tend to form vascular networks in softer gels vs. stiffer [52, 53], but the role of stiffness on endothelial cell differentiation is less clear. Data suggests that endothelial cells derived from different tissue sources may have different responses to scaffold properties [54]; this may be related to the

fact that EC characteristics vary according to native tissue type and function [55]. As pediatricc-kit+ CPCs in particular have not been studied extensively, the optimal conditions for their differentiation and maturation remain to be identified.

In regards to cardiac differentiation, we found no significant effect of elastic modulus on GATA4 or TNNT1 in either neonatal or adult ECM-based gels. It is possible that stiffer scaffolds may be necessary to induce cardiac differentiation of human CPCs. For example, the human fetal heart may be as stiff as 20 kPa [56], which is similar to the stiffest gel studied here (32 kPa). Mesenchymal stem cells had higher cardiac differentiation efficiency in 65 kPa gels compared to softer scaffolds [57]. Studying a wider range of elastic moduli will be critical. Our future work will aim to optimize cardiovascular differentiation of the CPCs by further tuning biochemical and mechanical properties of the hybrid gels. This will include exploring cardiac ECM from additional developmental time points (eg, fetal, older adult) as well as a broader range of scaffold mechanical properties. It will also be interesting to study other stem cell types with greater cardiac potential than c-kit+ CPCs, such as embryonic or induced pluripotent stem cells, in our hybrid gel system.

The cardiac ECM-fibrin hybrid scaffold presents a simple and robust approach to controlling biochemical and mechanical signals that direct cell fate. Scaffold mechanical properties are easily controlled using TG, which is highly compatible with cells. Additionally, scaffold composition can be tuned by adding ECM from various developmental ages, which has disparate effects on cell differentiation. Cells can be added directly to the scaffold solution to form a cell laden gel, and furthermore, the solution is easily injectable through a 25G needle even at the highest Young's modulus studied. Finally, ECM and fibrin are completely biodegradable without additional chemistry that is necessary for PEG-based or other synthetic biomaterials. Nevertheless, there are some limitations to our current study. In terms of the hybrid gel system, we were limited to a relatively low ECM: fibrin ratio (~1:10), as high concentrations of ECM inhibited gelation of the hybrid scaffold. Our rationale for ECM composition and stiffness range was based on our previous work studying the developing and mature rat myocardium [27, 34]. However, rat cardiac ECM may have some important differences compared to human cardiac ECM and thus may not be the optimal choice. Further work will search for an alternative ECM source that may better mimic the human myocardium both in terms of composition and stiffness. The ECM can influence cell response to soluble factors [11, 58], and thus exploring different culture medium formulations may also enhance cell differentiation. Fibrin itself is cell adhesive and is likely affecting CPC behavior in addition to the ECM. The influence of fibrin may not be a disadvantage, but its role should be clarified in future work. Indeed, many of the advantages of fibrin highlighted above make it an attractive scaffold "backbone". We also did not control fiber structure or orientation in our gels, although these variables can play an important role in cardiac cell differentiation and function [20, 59, 60]. Potential approaches in future studies could include varying calcium and thrombin concentrations [61], and controlling fibrin gel compaction or use of a magnetic field to induce alignment [62, 63].

Another potential limitation derives from the cell source, as the cells used in this study were isolated from a single patient and were highly heterogeneous in their marker expression (***Figure 3B***). It is possible that cells from another patient would have different responses,

and future work will seek to understand what role the heterogeneity of this cell population plays in the response of the cells to the hybrid gel with a particular focus on attempting to isolate a marker set that identifies cells that respond in a favorable manner for cardiac regeneration. We view the hybrid system described here as the first iteration in developing a biomimetic scaffold that can promote CPC differentiation towards cardiovascular lineages, and optimization in future scaffold designs will address the limitations described above. Moreover, as this hybrid system is designed to be used as an acellular injectable, we will seek to assess the effects of this hybrid gel system *in vivo* and, in particular, we will study the ability of resident cells of the heart to migrate into the scaffold in order to promote tissue growth/ regeneration in cardiac injury models.

5. Conclusion

We have developed a cardiac ECM-fibrin hybrid scaffold that has tunable composition and elastic moduli to mimic properties of the developing and mature myocardium. ECM of various developmental ages can be used and stiffness is controlled by crosslinking via TG with minimal effect on cell viability. Both cardiac ECM developmental age and stiffness of the scaffolds affected cardiovascular gene expression and network formation of c-kit+ CPCs from pediatric patients. In particular, the endothelial cell gene VWF and the smooth muscle gene CNN1 were up-regulated in the stiffest adult and neonatal ECM gels, respectively. In contrast, increasing the Young's modulus of the scaffolds significantly inhibited cellular network formation, suggesting different cues for pediatric c-kit+ CPC differentiation vs. maturation. The ECM-fibrin hybrid solutions were easily injectable through a 25G needle and formed gels *in situ*. Although we focused on cardiac ECM, the scaffold has potential to be adapted to a variety of other organs. Injectable ECM-based scaffolds with tunable properties that can direct progenitor cell fate and behavior will enhance future tissue engineering and regenerative medicine strategies.

Supplementary Material

Refer to Web version on PubMed Central for supplementary material.

Acknowledgments

This work was supported by the NRSA individual postdoctoral fellowship F32 HL112538 (C.W.), the Tufts University Biomedical Engineering Research Scholars (TUBERS) Program (E.B.), the NIH Pathway to Independence Award R00 HL093358 (L.D.B.), NIH-NHLBI Award R21 HL115570 (L.D.B.), and NSF CAREER Award NSF1351241 (L.D.B). We are grateful to Yuji Takeda and Professor Qiaobing Xu (Tufts University) for generously providing the transglutaminase. We also thank Kristin French and Professor Michael Davis (Georgia Institute of Technology/ Emory University) for helpful discussions and protocols on c-kit+ CPC isolation and characterization.

References

1. Go AS, Mozaffarian D, Roger VL, Benjamin EJ, Berry JD, Borden WB, Bravata DM, Dai S, Ford ES, Fox CS, Franco S, Fullerton HJ, Gillespie C, Hailpern SM, Heit JA, Howard VJ, Huffman MD, Kissela BM, Kittner SJ, Lackland DT, Lichtman JH, Lisabeth LD, Magid D, Marcus GM, Marelli A, Matchar DB, McGuire DK, Mohler ER, Moy CS, Mussolino ME, Nichol G, Paynter NP, Schreiner PJ, Sorlie PD, Stein J, Turan TN, Virani SS, Wong ND, Woo D, Turner MB,

o.b.o.t.A.H.A.S.C.a.S.S. Subcommittee. Heart disease and stroke statistics - 2013 update: a report from the American Heart Association. Circulation. 2013; 127:e6–e245. [PubMed: 23239837]

2. Kaushal S, Jacobs JP, Gossett JG, Steele A, Steele P, Davis CR, Pahl E, Vijayan K, Asante-Korang A, Boucek RJ, Backer CL, Wold LE. Innovation in basic science: Stem cells and their role in the treatment of paediatric cardiac failure - opportunities and challenges. Cardiol Young. 2009; 19(Suppl 2):74–84. [PubMed: 19857353]
3. Ye KY, Black LD. Strategies for tissue engineering cardiac constructs to affect functional repair following myocardial infarction. J Cardiovasc Trans Res. 2011; 4:575–591.
4. Schure AY, Kussman BD. Pediatric heart transplantation: demographics, outcomes, and anesthetic implications. Pediatr Anesth. 2011; 21:594–603.
5. Almond CSD, Thiagarajan RR, Piercey GE, Gauvreau K, Blume ED, Bastardi HJ, Fynn-Thompson F, Singh TP. Waiting list mortality among children listed for heart transplantation in the United States. Circulation. 2009; 119:717–727. [PubMed: 19171850]
6. Bolli R, Chugh AR, D'Amario D, Loughran JH, Stoddard MF, Ikram S, Beache GM, Wagner SG, Leri A, Hosoda T, Sanada F, Elmore JB, Goichberg P, Cappetta D, Salankhi NK, Fahsah I, Rokosh DG, Slaughter MS, Kajstura J, Anversa P. Cardiac stem cells in patients with ischaemic cardiomyopathy (SCIPIO): initial results of a randomised phase 1 trial. The Lancet. 2011; 378:1847–1857.
7. Mishra R, Vijayan K, Colletti EJ, Harrington DA, Mattiesen TS, Simpson D, Goh SK, Walker BL, Almeida-Porada G, Wang D, Backer CL, Dudley J. Samuel C. Wold LE, Kaushal S. Characterization and functionality of cardiac progenitor cells in congenital heart patients. Circulation. 2011; 123:364–373. [PubMed: 21242485]
8. Simpson DL, Mishra R, Sharma S, Goh SK, Deshmukh S, Kaushal S. A strong regenerative ability of cardiac stem cells derived from neonatal hearts. Circulation. 2012; 126(suppl 1):S46–S53. [PubMed: 22965993]
9. van_Berlo JH, Kanisicak O, Maillet M, Vagnozzi RJ, Karch J, Lin S-CJ, Middleton RC, Marban E, Molkentin JD. c-kit+ cells minimally contribute cardiomyocytes to the heart. Nature. 2014; 509:337–341. [PubMed: 24805242]
10. Hsieh PCH, Davis ME, Lisowski LK, Lee RT. Endothelial-cardiomyocyte interactions in cardiac development and repair. Annu Rev Physiol. 2006; 68:51–66. [PubMed: 16460266]
11. Zhang J, Klos M, Wilson GF, Herman AM, Lian X, Raval KK, Barron MR, Hou L, Soerens AG, Yu J, Palecek SP, Lyons GE, Thomson JA, Herron TJ, Jalife J, Kamp TJ. Extracellular matrix promotes highly efficient cardiac differentiation of human pluripotent stem cells: the matrix sandwich method. Circ Res. 2012; 111:1125–1136. [PubMed: 22912385]
12. French KM, Boopathy AV, DeQuach JA, Chingozha L, Lu H, Christman KL, Davis ME. A naturally derived cardiac extracellular matrix enhances cardiac progenitor cell behavior in vitro. Acta Biomaterialia. 2012; 8(12):4357–4364. [PubMed: 22842035]
13. Engler AJ, Sen S, Sweeney HL, Discher DE. Matrix elasticity directs stem cell lineage specification. Cell. 2006; 126:677–689. [PubMed: 16923388]
14. Young, J.L. and A.J. Engler Hydrogels with time-dependent material properties enhance cardiomyocyte differentiation in vitro. Biomaterials. 2011; 32:1002–1009. [PubMed: 21071078]
15. Greiner AM, Richter B, Bastmeyer M. Micro-engineered 3D scaffolds for cell culture studies. Macromol Biosci. 2012; 12:1301–1314. [PubMed: 22965790]
16. Singelyn JM, DeQuach JA, Seif-Naraghi SB, Littlefield RB, Schup-Magoffin PJ, Christman KL. Naturally derived myocardial matrix as an injectable scaffold for cardiac tissue engineering. Biomaterials. 2009; 30:5409–5416. [PubMed: 19608268]
17. Singelyn JM, Sundaramurthy P, Johnson TD, Schup-Magoffin PJ, Hu DP, Faulk DM, Wang J, Mayle KM, Bartels K, Salvatore M, Kinsey AM, DeMaria AN, Dib N, Christman KL. Catheter-deliverable hydrogel derived from decellularized ventricular extracellular matrix increases endogenous cardiomyocytes and preserves cardiac function post-myocardial infarction. J Am Coll Cardiol. 2012; 59(8):751–763. [PubMed: 22340268]
18. Seif-Naraghi SB, Singelyn JM, Salvatore MA, Osborn KG, Wang JJ, Sampat U, Kwan OL, Strachan GM, Wong J, Schup-Magoffin PJ, Braden RL, Bartels K, DeQuach JA, Preul M, Kinsey

AM, DeMaria AN, Dib N, Christman KL. Safety and efficacy of an injectable extracellular matrix hydrogel for treating myocardial infarction. Science Transl Med. 2013; 5:173ra25.

19. Grover GN, Rao N, Christman KL. Myocardial matrix-polyethylene glycol hybrid hydrogels for tissue engineering. Nanotechnol. 2014; 25:014011.
20. Black LD, Meyers JD, Weinbaum JS, Shvelidze YA, Tranquillo RT. Cell-induced alignment augments twitch force in fibrin gel-based engineered myocardium via gap junction modification. Tissue Eng. 2009; 15(10):3099–3108.
21. Janmey PA, Winer JP, Weisel JW. Fibrin gels and their clinical and bioengineering applications. J R Soc Interface. 2009; 6:1–10. [PubMed: 18801715]
22. Deponti D, Giancamillo AD, Mangiavini L, Pozzi A, Fraschini G, Sosio C, Domeneghini C, Peretti GM. Fibrin-based model for cartilage regeneration: tissue maturation from in vitro to in vivo. Tissue Eng Part A. 2012; 18(11, 12):1109–1122. [PubMed: 22316220]
23. Syedain ZH, Weinberg JS, Tranquillo RT. Cyclic distension of fibrin-based tissue constructs: evidence of adaptation during growth of engineered connective tissue. Proc Natl Acad Sci. 2008; 105(18):6537–6542. [PubMed: 18436647]
24. Lesman A, Koffler J, Atlas R, Blinder YJ, Kam Z, Levenberg S. Engineering vessel-like networks within multicellular fibrin-based constructs. Biomaterials. 2011; 32:7856–7869. [PubMed: 21816465]
25. Lafleur MA, Handsley MM, Knauper V, Murphy G, Edwards DR. Endothelial tubulogenesis within fibrin gels specifically requires the activity of membrane-type-matrix metalloproteinases (MT-MMPs). J Cell Sci. 2002; 115:3427–3438. [PubMed: 12154073]
26. Morin KT, Tranquilllo RT. In vitro models of angiogenesis and vasculogenesis in fibrin gel. Exp Cell Res. 2013; 319:2409–2417. [PubMed: 23800466]
27. Williams C, Quinn KP, Georgakoudi I, Black LD. Young developmental age cardiac extracellular matrix promotes the expansion of neonatal cardiomyocytes in vitro. Acta Biomater. 2014; 10(1): 194–204. [PubMed: 24012606]
28. Black LD, Brewer KK, Morris SM, Schreiber BM, Toselli P, Nugent MA, Suki B, Stone PJ. Effects of elastase on the mechanical and failure properties of engineered elastin-rich matrices. J Appl Physiol. 2005; 98:1434–1441. [PubMed: 15640390]
29. Black LD, Allen PG, Morris SM, Stone PJ, Suki B. Mechanical and failure properties of extracellular matrix sheets as a function of structural protein composition. Biophys J. 2008; 94:1916–1929. [PubMed: 17993498]
30. Tiwary AK, Rana V. Cross-linked chitosan films: effect of cross-linking density on swelling parameters. Pak J Pharm Sci. 2010; 23(4):443–448. [PubMed: 20884460]
31. He J-Q, Vu DM, Hunt G, Chugh A, Bhatnagar A, Bolli R. Human cardiac stem cells isolated from atrial appendages stably express c-kit. PLoS One. 2011; 6(11):e27719. [PubMed: 22140461]
32. Smits AM, Vliet P.v. Metz CH, Korfage T, Sluijter JPG, Doevendans PA, Goumans M-J. Human cardiomyocyte progenitor cells differentiate into functional mature cardiomyocytes: an in vitro model for studying human cardiac physiology and pathophysiology. Nature Protocols. 2009; 4(2): 232–243.
33. Singelyn JM, Christman KL. Modulation of material properties of a decellularized myocardial matrix scaffold. Macromol Biosci. 2011; 11(6):731–738. [PubMed: 21322109]
34. Gershlak JR, Resnikoff JI, Sullivan KE, Williams C, Wang RM, Black LD. Mesenchymal stem cells ability to generate traction stress in response to substrate stiffness is modulated by the changing extracellular matrix composition of the heart during development. Biochem Biophys Res Comm. 2013; 439:161–166. [PubMed: 23994333]
35. Jacot JG, Martin JC, Hunt DL. Mechanobiology of cardiomyocyte development. J Biomech. 2010; 43:93–98. [PubMed: 19819458]
36. Sundararaghavan HG, Monteiro GA, Lapin NA, Chabal YJ, Miksan JR, Shreiber DI. Genipin-induced changes in collagen gels: correlation of mechanical properties to fluorescence. J Biomed Mater Res. 2008; 87A:308–320.
37. Girton TS, Oegema TR, Tranquillo RT. Exploiting glycation to stiffen and strengthen tissue equivalents for tissue engineering. J Biomed Mater Res. 1999; 46:87–92. [PubMed: 10357139]

38. Greenberg CS, Birckbichler PJ, Rice RH. Transglutaminases: multifunctional cross-linking enzymes that stabilize tissues. FASEB J. 1991; 5(15):3071–3077. [PubMed: 1683845]
39. Misfeldt AM, Boyle SC, Tompkins KL, Bautch VL, Labosky PA, Baldwin HS. Endocardial cells are a distinct endothelial lineage derived from Flk1+ multipotent cardiovascular progenitors. Dev Biol. 2009; 333(1):78–89. [PubMed: 19576203]
40. Seif-Naraghi SB, Horn D, Schup-Magoffin PJ, Christman KL. Injectable extracellular matrix derived hydrogel provides a platform for enhanced retention and delivery of a heparin-binding growth factor. Acta Biomaterialia. 2012; 8:3695–3703. [PubMed: 22750737]
41. Singelyn JM, Christman KL. Injectable materials for the treatment of myocardial infarction and heart failure: The promise of decellularized matrices. J Cardiovasc Trans Res. 2010; 3:478–486.
42. Pok S, Jacot JG. Biomaterials advances in patches for congenital heart defect repair. J Cardiovasc Trans Res. 2011; 4(5):646–654.
43. Farhadian F, Contard F, Corbier A, Barrieux A, Rappaport L, Samuel JL. Fibronectin expression during physiological and pathological cardiac growth. J Mol Cell Cardiol. 1995; 27:981–990. [PubMed: 7563110]
44. Mays PK, McAnulty RJ, Campa JS, Laurent GJ. Age-related changes in collagen synthesis and degradation in rat tissues. Biochem J. 1991; 276:307–313. [PubMed: 2049064]
45. Jacot JG, McCulloch AD, Omens JH. Substrate stiffness affects the functional maturation of neonatal rat ventricular myocytes. Biophys J. 2008; 95:3479–3487. [PubMed: 18586852]
46. Engler AJ, Carag-Krieger C, Johnson CP, Raab M, Tang H-Y, Speicher DW, Sanger JW, Sanger JM, Discher DE. Embryonic cardiomyocytes beat best on a matrix with heart-like elasticity: scar-like rigidity inhibits beating. J Cell Sci. 2008; 121:3794–3802. [PubMed: 18957515]
47. Breuls RGM, Klumpers DD, Everts V, Smit TH. Collagen type V modulates fibroblast behavior dependent on substrate stiffness. Biochem Biophys Res Comm. 2009; 380:425–429. [PubMed: 19280692]
48. Lee J, Abdeen AA, Zhang D, Kilian KA. Directing stem cell fate on hydrogel substrates by controlling cell geometry, matrix mechanics and adhesion ligand composition. Biomaterials. 2013; 34:8140–8148. [PubMed: 23932245]
49. O'Brien XM, Loosley AJ, Oakley KE, Tang JX, Reichner JS. Introducing a novel metric, directionality time, to quantify human neutrophil chemotaxis as a function of matrix composition and stiffness. J Leukoc Biol. 2014 in press.
50. Schense JC, Hubbell JA. Cross-linking exogenous bifunctional peptides into fibrin gels with factor XIIIa. Bioconjugate Chem. 1999; 10:75–81.
51. Ali S, Saik JE, Gould DJ, Dickinson ME, West JL. Immobilization of cell-adhesion laminin peptides in degradable PEGDA hydrogels influences endothelial cell tubulogenesis. BioResearch Open Access. 2013; 2(4):241–249. [PubMed: 23914330]
52. Califano, JP.; Reinhart-King, CA. The effects of substrate elasticity on endothelial cell network formation and traction force generation. IEEE EMBS; 31st Annual International Conference; 2009. p. 3343-3345.
53. Hanjaya-Putra D, Yee J, Ceci D, Truitt R, Yee D, Gerecht S. Vascular endothelial growth factor and substrate mechanics regulate in vitro tubulogenesis of endothelial progenitor cells. J Cell Mol Med. 201; 14(10):2436–2447. [PubMed: 19968735]
54. Sieminski AL, Hebbel RP, Gooch KJ. The relative magnitudes of endothelial force generation and matrix stiffness modulate capillary morphogenesis in vitro. Exp Cell Res. 2004; 297(2):574–584. [PubMed: 15212957]
55. Luttun A, Carmeliet P. De novo vasculogenesis in the heart. Cardiovasc Res. 2003; 58:378–389. [PubMed: 12757872]
56. Ohayon J, Usson Y, Jouk PS, Cai H. Fibre orientation in human fetal heart and ventricular mechanics: a small perturbation. Comp Meth Biomech Biomed Eng. 1999; 2(2):83–105.
57. Li Z, Guo X, Palmer AF, Das H, Guan J. High-efficiency matrix modulus-induced cardiac differentiation of human mesenchymal stem cells inside a thermosensitive hydrogel. Acta Biomater. 2012; 8(10):3586–3595. [PubMed: 22729021]

58. Ieda M, Tsuchihashi T, Ivey KN, Ross RS, Hong TT, Shaw RM, Srivastava D. Cardiac fibroblasts regulate myocardial proliferation through beta1 integrin signaling. Dev Cell. 2009; 16:233–244. [PubMed: 19217425]

59. Liau B, Christoforou N, Leong KW, Bursac N. Pluripotent stem cell-derived cardiac tissue patch with advanced structure and function. Biomaterials. 2011; 32(35):9180–9187. [PubMed: 21906802]

60. Pijnappels DA, Schalij MJ, Ramkisoensing AA, Tuyn J.v. Vries A.A.F.d. Laarse A.v.d. Ypey DL, Atsma DE. Forced alignment of mesenchymal stem cells undergoing cardiomyogenic differentiation affects functional integration with cardiomyocyte cultures. Circ Res. 2008; 103:167–176. [PubMed: 18556577]

61. Ryan EA, Mockros LF, Weisel JW, Lorand L. Structural origins of fibrin clot rheology. BIophys J. 1999; 77:2813–2826. [PubMed: 10545379]

62. Girton TS, Dubey N, Tranquillo RT. Magnetic-induced alignment of collagen fibrils in tissue equivalents. Methods Mol Med. 1999; 18:67–73. [PubMed: 21370168]

63. Morin KT, Tranquillo RT. Guided sprouting from endothelial spheroids in fibrin gels aligned by magnetic fields and cell-induced gel compaction. Biomaterials. 2011; 32:6111–6118. [PubMed: 21636127]

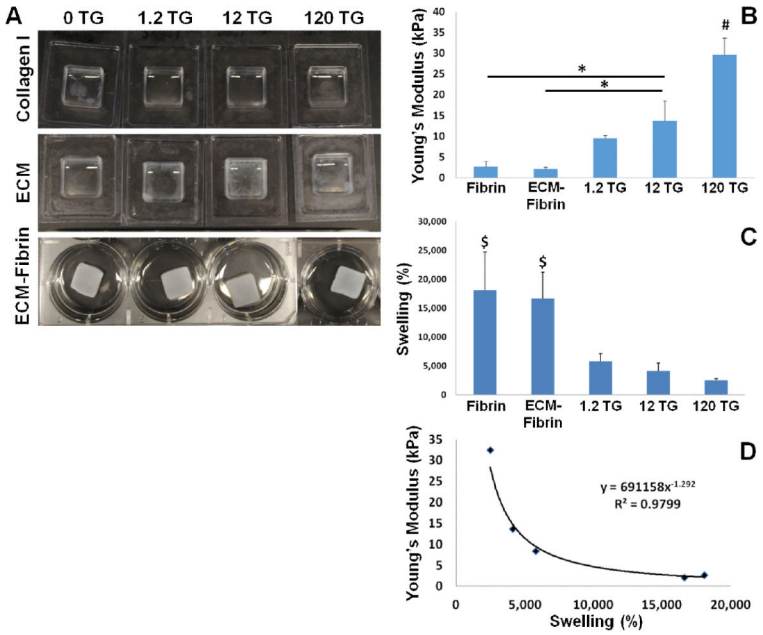

Figure 1. Characterization of ECM-Fibrin hybrid gels

(A) Representative macroscopic images of Collagen I (*top*), adult cardiac ECM (*middle*), and ECM-fibrin gels (*bottom*) crosslinked with increasing amounts of TG. TG did not crosslink Collagen I. Although some crosslinking occurred in ECM gels, the process was incomplete and gels remained mostly fluid. The combination of ECM with fibrin led to the formation of hydrogels with mechanical strength. (B) Young's Modulus of gels determined by uniaxial testing shows increasing stiffness with increasing TG. (C) Swell ratio decreases with increasing TG. (D) Young's modulus strongly correlates with swelling by power law fit. # = significantly different vs. all; *$* = significantly different vs. all TG crosslinked for $p < 0.05$ (N = 4 per condition).

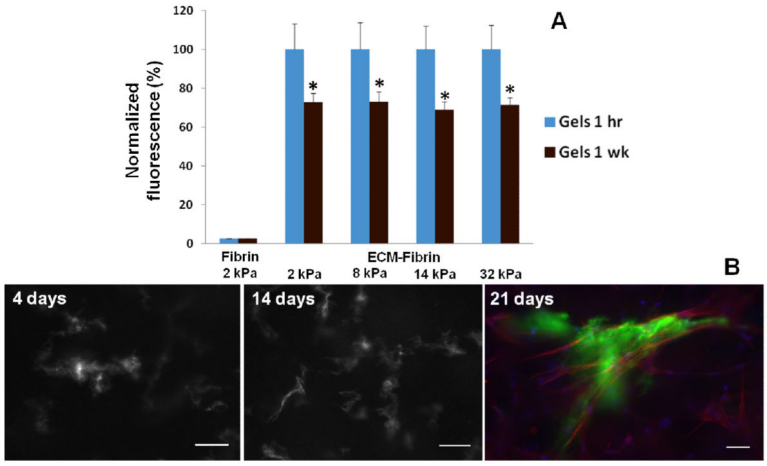

Figure 2. ECM retention within hybrid gels

(A) Gels containing Alexa Fluor 488 labeled ECM had similar levels 1 hr after gelling. After 1 wk incubation with PBS, fluorescence levels within gels significantly decreased from corresponding baseline levels but were similar in all gels regardless of TG crosslinking. Fluorescence values are normalized to baseline levels at 1 hr (N = 6 per condition). (B) Representative images of AF488 labeled adult ECM-fibrin hybrid gels crosslinked with 1.2 μg/ml TG. ECM becomes more concentrated and fibers become apparent, suggestive of cell interaction and remodeling. Day 21 shows ECM (*green*), cells labeled with TRITC-phalloidin (*red*) and Hoechst stain for nuclei (*blue*). Scale bars = 25 μm.

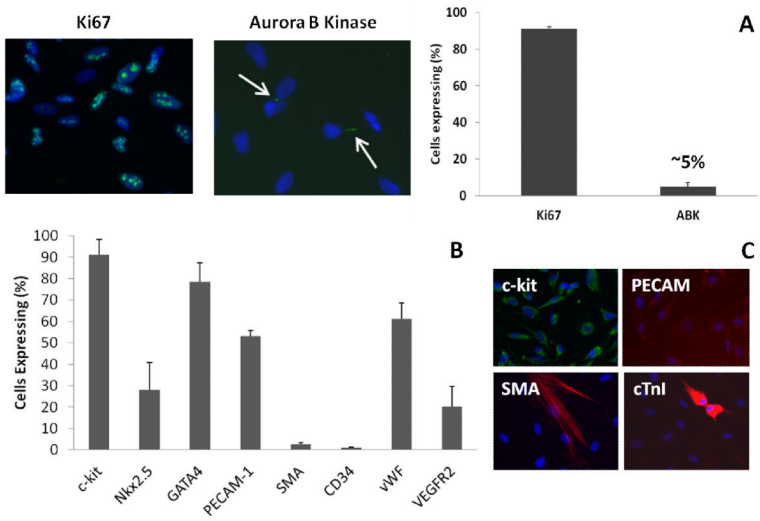

Figure 3. Characterization of c-kit+ cells

(A) Staining for Ki67 (mitosis marker) and Aurora B Kinase (ABK; cytokinesis marker) shows that c-kit+ cells are highly proliferative. (B) Analysis of various markers in c-kit+ cells at passage 4. (C) At higher passages, cells spontaneously express markers for the three cardiovascular lineages: PECAM-1, smooth muscle α-actin (SMA), and cardiac troponin I (cTnI). N = 4 per condition.

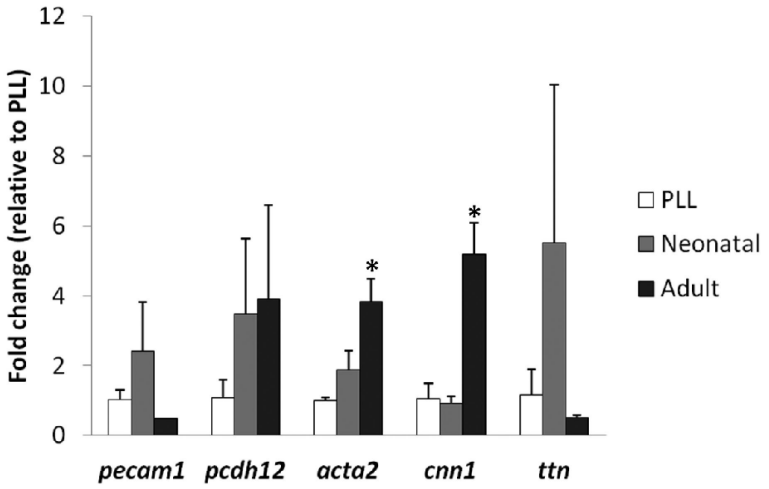

Figure 4. Gene expression on cardiac ECM

c-kit+ cells cultured on poly-L-lysine (PLL), neonatal ECM, or adult ECM were assayed after 21 days by PCR for endothelial (*pecam1*, *pcdh12*), smooth muscle (*acta2*, *cnn1*), and cardiac (*ttn*) genes. There was significant up-regulation of smooth muscle genes on adult cardiac ECM compared to PLL and neonatal ECM. * = significant difference compared to PLL and neonatal ECM for $p < 0.05$ (N = 4 per condition).

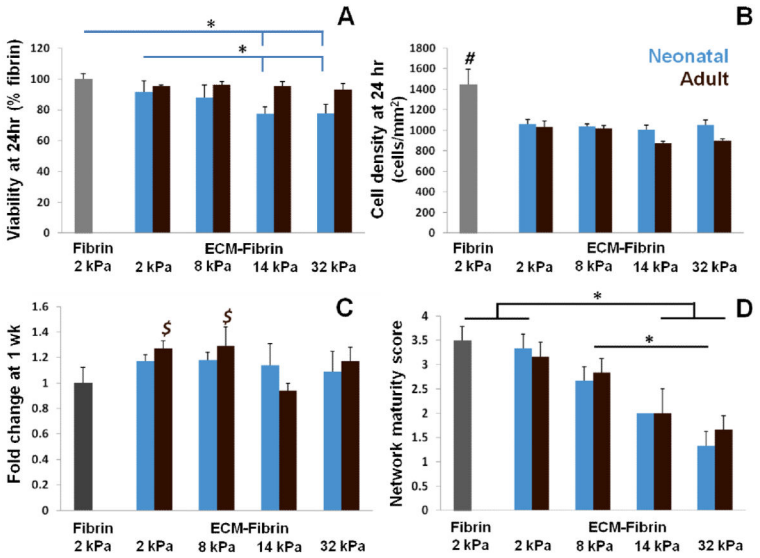

Figure 5. Cell measurements in ECM-Fibrin gels

(A) Cell viability was significantly lower in 14 kPa (12 μg/ml TG) and 32 kPa (120 μg/ml TG) neonatal ECM-fibrin gels compared to 2 kPa (0 TG) fibrin and ECM-fibrin gels. Cell viability was not significantly affected in adult ECM-fibrin gels crosslinked with TG. (B) Cells were significantly more dense in 2 kPa fibrin control gels compared to all other conditions at 24 hr. (C) Cell numbers increased modestly but significantly in 2 kPa and 8 kPa adult ECM gels compared to 2 kPa fibrin and 14 kPa adult ECM gels. Cell numbers did not change significantly in neonatal ECM-based gels. (D) Network scoring shows a decrease in network formation with increasing Young's modulus regardless of ECM age. # = significant difference vs. all other conditions; $ = significant difference vs. 2 kPa fibrin and 8 kPa ECM-fibrin for $p < 0.05$ (N = 3-5 per condition).

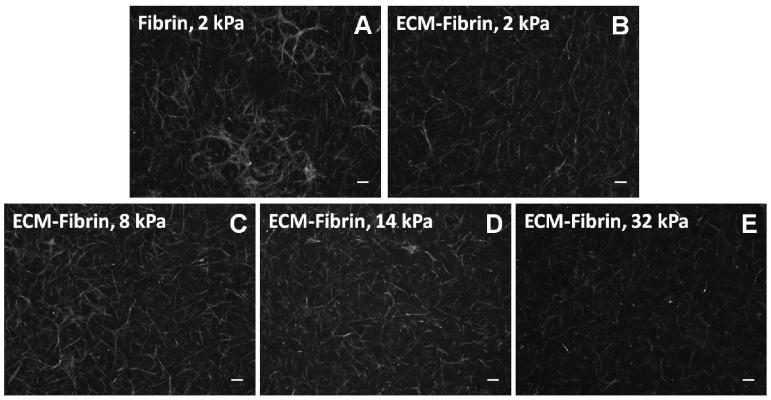

Figure 6. Cell morphology in ECM-Fibrin gels at 1 wk

Examples of Phalloidin staining of cells in adult ECM hybrid gels shown. Greater network formation is evident in softer gels than those with higher Young's moduli (quantified in Figure 5D). Scale bars = 100 μm.

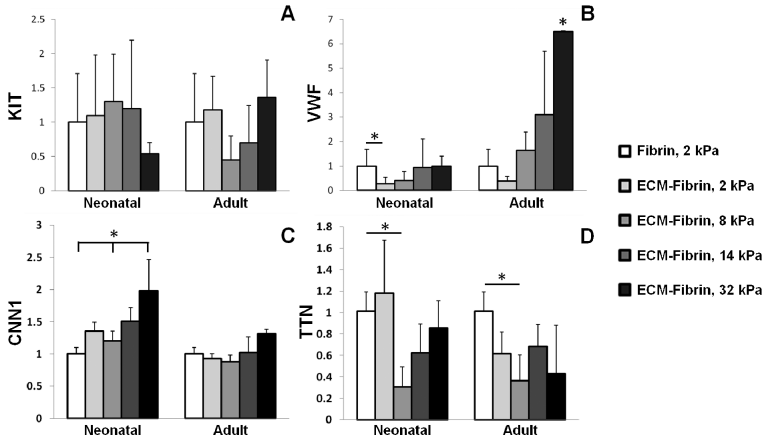

Figure 7. Cardiovascular gene expression in ECM-fibrin gels at 21 days

(A) ECM age and Young's modulus did not significantly affect the expression of KIT. (B) The endothelial cell marker VWF was significantly down-regulated in 2 kPa neonatal ECM-fibrin gels but significantly up-regulated in 32 kPa adult ECM gels compared to softer conditions. (C) The smooth muscle marker CNN1 was significantly up-regulated in 32 kPa neonatal ECM-fibrin gels compared to 2 kPa fibrin controls and 8 kPa neonatal ECM-fibrin. (D) The cardiac marker TTN was significantly down-regulated in 8 kPa neonatal and adult-based gels. * = significant difference for $p < 0.05$ (N = 3-4 per condition).

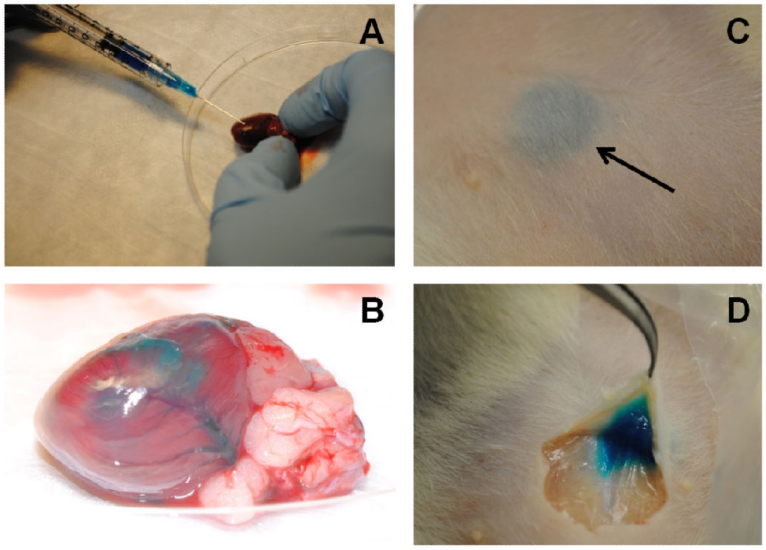

Figure 8. Injectability of ECM-fibrin gels

(A) ECM-Fibrin mixture with or without TG cross-linker can be drawn up into a syringe with a 25G needle and injected into rat left ventricular myocardium. (B) Blue dye added to the ECM-fibrin mixture shows perfusion through coronary arteries and into the surrounding tissue. (C) Subcutaneous injection shows the formation of a bolus under the skin (arrow). (D) Twenty minutes after injection, an incision was made to reveal formation of the gel. Example images are shown for 32 kPa gels (120 μg/ml TG) with adult ECM.